RESEARCH PAPERS

Acta Cryst. (1994). B**50**, 261–268

Structure of a Modulated Monoclinic Phase of $Na_4TiP_2O_9$

By B. A. Maximov, N. B. Bolotina and V. I. Simonov

Institute of Crystallography, Academy of Sciences of Russia, Leninsky pr. 59, 117333 *Moscow, Russia*

and V. Petříček

Institute of Physics, Academy of Sciences of the Czech Republic, Na Slovance 2, 180 40 *Praha* 8, *Czech Republic*

and H. Schulz

Institut für Kristallographie und Mineralogie der Universität München, Theresienstrasse 41, 8000 *München* 2, *Germany*

(*Received* 24 *April* 1993; *accepted* 17 *September* 1993)

Dedicated to Professor E. F. Bertaut on the occasion of his 80*th birthday*

Abstract

The crystal structure of tetrasodium titanium nonaoxodiphosphate, $Na_4TiP_2O_9$, has been investigated at 293 K from X-ray diffraction data collected on a CAD-4*F* diffractometer using Cu $K\alpha$ radiation, λ = 1.5418 Å. The structure is commensurately modulated monoclinic, with the basic cell parameters: $a = 8.631$ (1), $b = 7.541$ (1), $c = 7.049$ (1) Å, $\beta = 116.10$ (2)°, $Z = 2$. The superspace group is $P^{P2/c}_{\bar{1}\,s}$; the wavevector is $\mathbf{q} = 0.2\mathbf{a}^* + 0.2\mathbf{c}^*$. D_x = 2.786 Mg m^{-3}; $M_r = 345.779$; μ(Cu $K\alpha$) = 15.202 mm^{-1}; $F(000) = 336$. The final R factors are as follows: $R = 0.080$ for all 3056 reflections, R_0 = 0.068 for 729 main Bragg reflections, $R_1 = 0.076$ for 1329 first-order satellite reflections, $R_2 = 0.113$ for 998 second-order satellite reflections. The crystal structure of $Na_4TiP_2O_9$ at 293 K consists of $\{Ti_2[PO_4]_4O_2\}_\infty$ chains parallel to the [001] direction. The voids between the chains are occupied by Na atoms. The positions of these Na atoms, which in superionic high-temperature modifications of $Na_4TiP_2O_9$ are involved in ionic transport, have been studied in detail. Unlike the superionic phases, where the sites of these atoms are occupied statistically, in the monoclinic phase these sites are either unoccupied or fully occupied. The latter leads to the filling of the main conductivity channels, which causes the loss of conductivity in the monoclinic phase.

Introduction

$Na_4TiP_2O_9$ (NTP) crystals belong to a group of superionic conductors with Na ion conductivity (Matsajuki, Katsu & Simmi, 1983; Ivanov-Shits & Sigaryov, 1990). Above 573 K, the conductivity σ measured on polycrystalline samples is $2.6 \times 10^{-2}\ \Omega^{-1}$ cm^{-1}, while the activation energy is $E_a \simeq 0.33$ eV. A superionic phase transition occurs in the temperature range 520–540 K. Above 540 K, the ionic conductivity increases by more than an order of magnitude, while E_a decreases by a factor of approximately 0.5. Such a phase transition is apparently due to significant changes in the crystal structure. A considerable change in E_a may result from structural transformations which lead to smaller potential barriers between atomic sites involved in ionic transport. Structural studies at temperatures above and below this phase transition are required to analyse the structural changes accompanying it.

The first structural study of NTP crystals was performed at 573 K (Maximov, Klokova, Verin & Timofeeva, 1990). The superionic phase has orthorhombic symmetry; $a = 15.647$ (8), $b = 14.989$ (8), $c = 7.081$ (5) Å, space group *Ibam*, $Z = 8$. All previous attempts to solve the crystal structure, which is stable at room temperature, below the temperature of the superionic phase transition were unsuccessful. This might be due to the monoclinic phase of $Na_4TiP_2O_9$, which is stable at room temperature [a = 8.631 (1), $b = 7.541$ (1), $c = 7.049$ (1) Å, β = 116.10 (2)°], being modulated and twinned by pseudomerohedry. Therefore, analysis of the diffraction pattern from such samples becomes rather complicated. A preliminary description of the regularities of twinning laws and the geometry of the positions of satellite reflections is given by Maximov, Bolotina & Schulz (1994). The results of a full structural study of

©1994 International Union of Crystallography
Printed in Great Britain – all rights reserved

ISSN 0108-7681 ©1994

these crystals are presented below. Specific features of the structure of the modulated phase of monoclinic NTP crystals and the structural changes which occur in these crystals during the phase transition are discussed. X-ray diffraction patterns from a microtwinned sample of the modulated phase and the procedure used for the determination and refinement of the structural parameters of such a phase are also presented.*

* A list of structure factors has been deposited with the British Library Document Supply Centre as Supplementary Publication No. SUP 71811 (22 pp.). Copies may be obtained through The Technical Editor, International Union of Crystallography, 5 Abbey Square, Chester CH1 2HU, England.

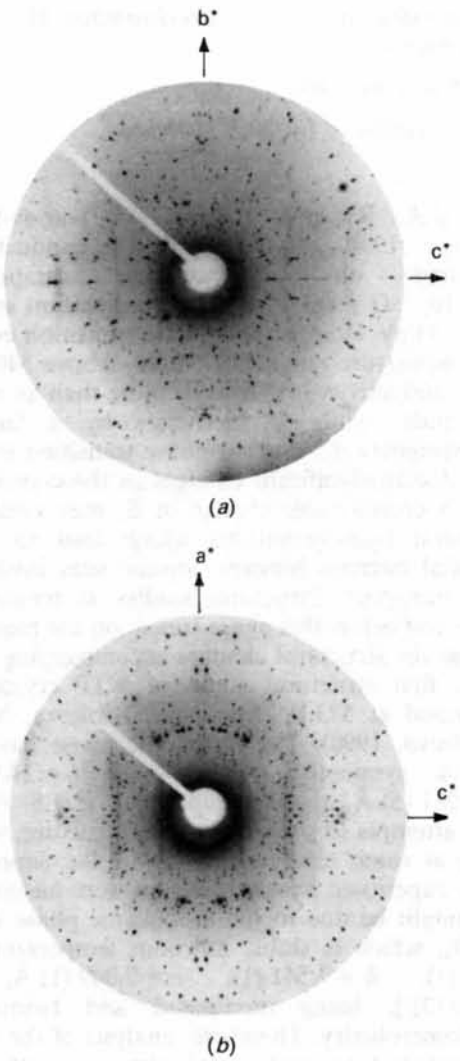

Fig. 1. Laue photographs of the monoclinic (pseudoorthorhombic) phase of microtwinned $Na_4TiP_2O_9$ crystals (Mo $K\alpha$ radiation, 293 K). The pseudoorthorhombic axes are denoted: (*a*) the primary X-ray beam parallel to the [100] direction; (*b*) the primary X-ray beam parallel to the [010] direction.

X-ray experiment and microtwinning

The crystals were synthesized by solution-melt crystallization in the Na_2CO_3–TiO_2–$NH_4H_2PO_4$ system. A crystal sphere of diameter 0.15 mm was used for the X-ray measurements. The diffraction patterns from NTP crystals of the monoclinic modification studied here are quite complicated due to both twinning and a large number of superstructure (satellite) reflections. The complexity of the diffraction pattern due to modulation and twinning is at a maximum when the primary beam lies in the twinning plane. Figs. 1(*a*) and 1(*b*) present such a Laue case. The diffraction patterns shown in Fig. 1 are quite complex, even more so due to significant diffuse scattering. The diffuse scattering is located in the (00*n*) planes ($n = 2,4,6,\ldots$) and may be caused by unoccupied Na sites or the uncorrelated thermal vibrations of atomic chains along the [001] direction. Precession photographs of the (*h*0*l*) (*h*1*l*) and (*h*2*l*) layers enabled the determination of the true symmetry of the NTP crystals at room temperature and the establishment of the twinning law and geometry of satellite reflections. A precession photograph of (*h*1*l*) is presented in Fig. 2(*a*).

Thus, it has been shown that at room temperature the NTP crystals are monoclinic and characterized by a superstructure and additional microtwinning

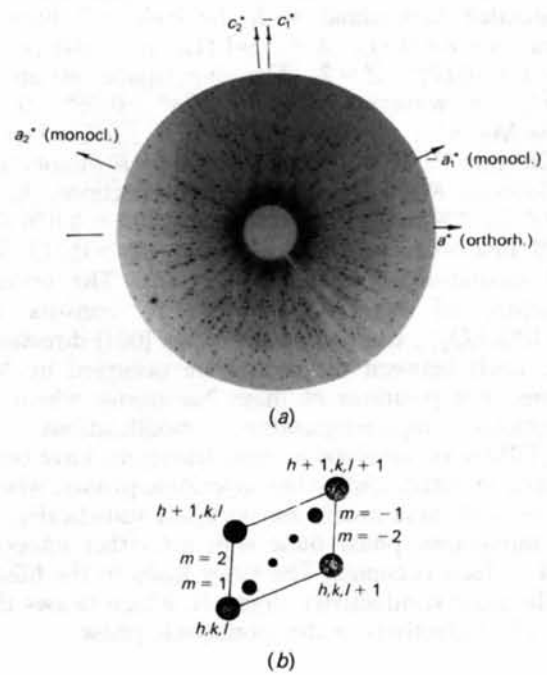

Fig. 2. The diffraction pattern of (*h*1*l*) from an $Na_4TiP_2O_9$ crystal: (*a*) precession photograph of the *h*1*l* layer (Mo $K\alpha$ radiation); (*b*) schematic arrangement of the superstructure reflections (small solid circles), $m = 1$ and 2, with reference to the main reflections (large solid circles).

with the following parameters for the basic monoclinic cell: $a_M = 8.631$ (1), $b_M = 7.541$ (1), $c_M = 7.049$ (1) Å, $\beta_M = 116.10$ (2)°. The lattice parameters were refined by the least-squares method using 25 reflections collected on a CAD-4*F* diffractometer. The superstructure reflections are indexed by the vectors $\mathbf{H} = h\mathbf{a}^* + k\mathbf{b}^* + l\mathbf{c}^* + m\mathbf{q}$, where $\mathbf{q} = 0.2\mathbf{a}^* + 0.2\mathbf{c}^*$, $m = 1.2$ (Fig. 2*b*). In this paper, the structure of NTP is interpreted as commensurately modulated. In accordance with the terminology adopted for the description of modulated structures, we shall refer to the vector $\mathbf{q}$ as the wavevector or the modulation vector, the reflections with $m = 0$ the main reflections and the reflections with $m = 1$ and 2 the first- and second-order satellites, respectively.

In order to understand the character of microtwinning, it should be taken into consideration that it is possible to pass from the monoclinic to the pseudoorthorhombic cell: $\mathbf{a}_R = 2\mathbf{a}_M + \mathbf{c}_M$, $a_R = 15.548$, $b_R = b_M = 7.541$, $c_R = c_M = 7.049$ Å, $\beta_R = 92.21°$. According to Friedel's classification, twinning by pseudomerohedry with index 1 occurs (Friedel, 1964). The twin plane *XY* of the othorhombic cell gives rise to two pseudomerohedric orthorhombic cells which diverge along the *z* direction, creating an angle of 4.42°, or, in the monoclinic description, two monoclinic twin partners related by the 2_z axis. The twinning law for the monoclinic description is $h_2 = h_1 + l_1$, $k_2 = -k_1$, $l_2 = -l_1$ (Fig. 2*a*). Only the $hk2\bar{h}$ reflections fully overlap in reciprocal space, while all other reflections, main and satellite, are split. The reflections lie so dense in the reciprocal space that their intensities are affected by their twin partners, if the X-ray measurements are made without optimization. Examination of the reflection profiles obtained without optimization revealed a large number of double peaks or strongly distorted profiles. We applied the following technique for optimization of the measurements. Prior to measuring the integral intensity of each reflection, the sample was rotated about the normal to the reflecting plane by an angle φ, so that both the diffraction vector $\mathbf{H}$ of the reflection to be measured and the nearest diffraction vector $\mathbf{H}'$ of the other twin partner are located in the equatorial plane of the diffractometer. In this orientation their diffraction profiles are as far apart from each other as possible over the ω angle; the reflections are in the optimum position for separate measurements. Thus, we managed to separate almost all the reflections and obtain the data for them, with the exception of the $hk2\bar{h}$ range, as expected. We have written a program, *PSIOPT*, to calculate the optimum values of φ rotations. A specific sequence of measurements was chosen for each twin partner. The main reflections ($m = 0$) were measured first, followed by the reflections of the superstructure cell: $5a_M = 43.155$, $b_M = 7.541$, $5c_M = 35.245$ Å, $\beta_M = 116.10°$. The ranges of h, k, l in the supercell were as follows: $-45 \le h \le 45$, $0 \le k \le 9$, $-40 \le l \le 40$; the variation among the standard reflections was no more than 1%. The maximum value of $\sin\theta/\lambda = 0.63$ Å^{-1} is due to the construction limitations of the diffractometer and caused by Cu $K\alpha$ radiation. Almost all the reflections were measured using the $\omega/2\theta$ scan mode. If for any reflection our calculations gave an insufficient separation of the twin partners for an $\omega/2\theta$ scan, the same calculations were then made for an ω scan. If that calculation yielded a better result, an ω scan of the reflection was made.

An array of the indexes h,k,l,m and structure factors $|F|_{obs}$ from one of the twin partners was used in the refinement of the structure. The reflections of the $hk2\bar{h}$-type were processed taking into account the following considerations: overlapping reflections of such a type are equivalent; a twin volume ratio of 1:1 was estimated from the intensities of the two different partners. Therefore, in the kinematic approximation the integrated intensities of these reflections can be halved and used, along with the other reflections, for the refinement procedure. The data set contained 1377 observed $[I > 3\sigma(I)]$ main reflections, including 37 reflections of the $hk2\bar{h}$ type and 4085 satellite reflections. An absorption correction for a sphere was applied. After averaging the symmetry-equivalent reflections, the data set contained 729 main reflections, with an internal R factor of 0.038, and 2327 satellite reflections, consisting of 1329 first-order and 998 second-order satellites. The internal R factor of the satellite reflections was 0.076. The main crystal data for the sample, experimental parameters, results of the averaging and all subsequent refinements are listed in Table 1.

Refinement of the structure parameters

As shown by de Wolff (1974) and de Wolff, Janssen & Janner (1981), it is possible to consider a modulated crystal as a three-dimensional section of a periodic supercrystal in (3 + 1)-dimensional space. A structure-factor formalism for modulated structures (de Wolff, 1974; Yamamoto, 1982) has been derived by Petříček, Coppens & Becker (1985). The program *JANA* (Petříček, Coppens & Becker, 1985; Petříček, 1993) was used for the refinement of the modulated structure. The average structure was refined first, using only the main reflections. Because of the conditions for observed reflections of the type $h0l$: $l = 2n$, the space groups were restricted to the centrosymmetric group $P2/c$ and non-centrosymmetric group Pc. The results of the refinement of the average structure with 729 main reflections yielded the following unweighted and weighted R factors: in space group

Table 1. *Crystal and experimental data*

Formula	$Na_4TiP_2O_9$			
Temperature (K)	293			
(3 + 1)-Dimensional space group	$P^{P2/c}_{1\,s}$			
Lattice parameters of the basic cell	a = 8.631 (1) Å			
	b = 7.541 (1) Å			
	c = 7.049 (1) Å			
	β = 116.10 (2)°			
Number of formula units per unit cell	$Z = 2$			
Calculated density D_x (Mg m^{-3})	2.786			
Twinning law	$h_2 = h_1 + l_1 \quad k_2 = -k_1 \quad l_2 = -l_1$			
Modulation vector	$\mathbf{q} = 0.2\mathbf{a}^* + 0.2\mathbf{c}^*$			
Experimental data				
Diffractometer	Enraf–Nonius CAD-4*F*			
Radiation, wavelength (Å)	Cu $K\alpha$, 1.5418			
Linear absorption coefficient (mm^{-1})	15.202			
Sample shape	Sphere			
Diameter (mm)	0.15			
Maximum sin θ/λ (Å^{-1})	0.63			
Region of measurements	Semisphere ($k \geq 0$)			
Parameters of structure refinement				
Functional minimized	$\sum w(\lvert F_{obs}\rvert - \lvert F_{calc}\rvert)^2$			
Weighting scheme	$w = 1/\sigma^2_F$			
Number of independent atoms	11			
Number of refined parameters	184			
Reflections	$\sum$	$hkl0$	$hkl \pm 1 + hkl \pm 2$	
Number of reflections observed	5462	1377	4085	
Criterion for significance	$I > 3\sigma(I)$			
R factor of equivalent averaging	–	0.038	0.076	
Number of averaged reflections	3056	729	1329	998
R factors of the refinement of the structure				
R	0.080	0.068	0.076	0.113
wR	0.091	0.084	0.097	0.107

$P2/c$, $R = 0.103$, $wR = 0.103$; in space group Pc, $R = 0.106$, $wR = 0.109$.

As there are second-order satellites in the diffraction pattern, a positional or occupational modulation wave of a particular atom, describing its displacement or occupancy variation, can be expressed as a Fourier sum of two harmonics

$$u_j = \sum_{k=1}^{2} (u^{(1)}_{jk} \sin 2\pi k\mathbf{q}\cdot\mathbf{r}_j + u^{(2)}_{jk} \cos 2\pi k\mathbf{q}\cdot\mathbf{r}_j),$$

where u_j is the value of variation, j is the number of the atom, k is the number of the harmonic, $\mathbf{q}$ is the wavevector and $\mathbf{r}_j$ is the average position of atom j. The amplitudes $u^{(1)}_{jk}$ and $u^{(2)}_{jk}$ are the parameters to be refined (Petříček, Coppens & Becker, 1985). In the two-harmonic approximation, an atom in a general position has 12 displacive and four occupancive modulation parameters (if the occupancy modulation exists, of course). For a given (3 + 1)-dimensional space group, the values of the modulation parameters are restricted when an atom is located at a special position of the basic three-dimensional space group (Petříček & Coppens, 1988). The condition for the $h0lm$ reflections is $l + m = 2n$. For a planar orientation of the vector $\mathbf{q} = 0.2\mathbf{a}^*_M + 0.2\mathbf{c}^*_M$, this does not contradict the two (3 + 1)-dimensional space groups $P^{P2/c}_{1\,s}$ and P^{Pc}_{s}. These groups do not correspond to the standard setting of de Wolff, Janssen & Janner (1981). In order to pass to the standard groups $P^{P2/b}_{1\,1}$ and P^{Pb}_{1}, it is necessary to perform two formal transformations: pass to a wavevector $\mathbf{q}' = 0.8\mathbf{a}^*_M + 0.8\mathbf{c}^*_M$ and then exchange the **b** and **c** axes. These groups are also represented in *International Tables for X-ray Crystallography* (1992, Vol. C) by the symbols $P2/b(\alpha\beta 0)$ and $Pb(\alpha\beta 0)$, respectively. However, the new vector $\mathbf{q}'$ crosses a boundary of the Brillouin zone, which is the reason for the choice of a non-standard but physically correct setting.

The refinement of the structure in both (non-standard) groups was made using a new version of the *JANA* program system (Petříček, 1992), supplemented by computational procedures intended for commensurately modulated structures. From this value, it is now possible to depict a value t_0 of the extra coordinate t (de Wolff, 1974) for the section of the (3 + 1)-dimensional space defined by a three-dimensional hyperplane t_0 = const. Unlike the incommensurately modulated structures, where t is any real value, in the commensurately modulated structures t changes discretely, with a constant interval (Yamamoto, 1982), and the values of t depend on the choice of 'zero-reading' t_0. In different t sections the positions of the atoms in a three-dimensional supercell are different. Moreover, different t sections can possess different three-dimensional superstructural symmetry, especially when the operators of the (3 + 1)-dimensional symmetry contain those which change the sign of the fourth coordinate. It is possible to show that for the centrosymmetric space group $P^{P2/c}_{1\,s}$, there are only two sections, $t_0 = 0$ and 1/2, which retain in the superstructural cell all the symmetry elements corresponding to the three-dimensional components of the (3 + 1)-dimensional symmetry. The refinement of the structure in this space group at $t_0 = 0$ yielded an R factor of *ca* 30% for second-order satellites, while at $t_0 = 1/2$ the following unweighted and weighted R factors of the refinement were obtained: $R = 0.080$, $wR = 0.091$ for all 3056 reflections; $R_0 = 0.068$, $wR_0 = 0.084$ for 729 main reflections; $R_1 = 0.076$, $wR_1 = 0.097$ for 1329 first-order satellite reflections; $R_2 = 0.113$, $wR_2 = 0.107$ for 998 second-order satellite reflections. An isotropic extinction parameter was used in the refinement, indicating that extinction effects are insignificant because even for the strongest reflections the correction factor was no less than 0.90, while for the others the value was close to 0.99. This is separate evidence of the high imperfection of the structure of the title crystals. In the noncentrosymmetric space group P^{Pc}_{s}, the R factors of the refinement are slightly smaller ($R = 0.075$, $R_0 = 0.063$, $R_1 = 0.071$, $R_2 = 0.112$), due to a significantly larger number of refined parameters (372 parameters instead of 184 parameters in the centrosymmetric space group). This observation, as well as strong

Table 2. *Structure of* $Na_4TiP_2O_9$: *coordinate* ($\bar{p}$), *modulation* (A_p) *and anisotropic thermal* (u_{ij}) *parameters*

$$\mathbf{p} = \mathbf{p} + \sum_{k=1}^{2} (A_p \sin \alpha_k + A_p \cos \alpha_k), \text{ where } \alpha_k = 2\pi \mathbf{q}.\mathbf{r};\ \mathbf{r} = (\bar{x}, \bar{y}, \bar{z}).$$

	Parameter	$p = x$	$p = y$	$p = z$	$p = \mu$
Ti	$\bar{p}$	$\frac{1}{2}$	$\frac{1}{2}$	0	1
	$A_p \sin(\alpha_1)$	0.0036 (2)	0.0408 (2)	0.0036 (4)	0
	$A_p \cos(\alpha_1)$	0	0	0	0
	$A_p \sin(\alpha_2)$	−0.0015 (3)	0.0004 (2)	−0.0040 (5)	0
	$A_p \cos(\alpha_2)$	0	0	0	0
	u_{11}, u_{22}, u_{33}	0.0069 (5)	0.0142 (6)	0.0179 (6)	
	u_{12}, u_{13}, u_{23}	−0.0002 (4)	0.0055 (5)	−0.0118 (4)	
P	$\bar{p}$	0.2399 (1)	0.2466 (1)	0.6042 (2)	1
	$A_p \sin(\alpha_1)$	−0.0081 (2)	0.0408 (2)	−0.0178 (4)	0
	$A_p \cos(\alpha_1)$	0.0177 (2)	−0.0012 (2)	0.0398 (4)	0
	$A_p \sin(\alpha_2)$	−0.0002 (2)	−0.0021 (2)	−0.0003 (4)	0
	$A_p \cos(\alpha_2)$	−0.0024 (2)	0.0020 (2)	−0.0057 (4)	0
	u_{11}, u_{22}, u_{33}	0.0101 (5)	0.0049 (5)	0.0096 (5)	
	u_{12}, u_{13}, u_{23}	−0.0026 (4)	0.0086 (4)	−0.0027 (4)	
O1	$\bar{p}$	$\frac{1}{2}$	0.6044 (5)	$\frac{3}{4}$	1
	$A_p \sin(\alpha_1)$	0	0.0423 (8)	0	0
	$A_p \cos(\alpha_1)$	−0.0054 (8)	0	−0.016 (1)	0
	$A_p \sin(\alpha_2)$	−0.0066 (9)	0	−0.012 (2)	0
	$A_p \cos(\alpha_2)$	0	−0.0003 (8)	0	0
	u_{11}, u_{22}, u_{33}	0.014 (2)	0.006 (2)	0.011 (2)	
	u_{12}, u_{13}, u_{23}	0	0.011 (2)	0	
O2	$\bar{p}$	0.6525 (4)	0.6940 (4)	0.1637 (7)	1
	$A_p \sin(\alpha_1)$	−0.0017 (6)	0.0369 (6)	−0.002 (1)	0
	$A_p \cos(\alpha_1)$	−0.0104 (6)	−0.0036 (6)	−0.029 (1)	0
	$A_p \sin(\alpha_2)$	−0.0033 (7)	0.0018 (6)	−0.005 (1)	0
	$A_p \cos(\alpha_2)$	−0.0010 (7)	0.0033 (6)	−0.002 (1)	0
	u_{11}, u_{22}, u_{33}	0.022 (2)	0.009 (1)	0.013 (1)	
	u_{12}, u_{13}, u_{23}	−0.008 (1)	0.015 (1)	−0.007 (1)	
O3	$\bar{p}$	0.2935 (4)	0.6428 (4)	−0.0440 (7)	1
	$A_p \sin(\alpha_1)$	0.0030 (6)	0.0423 (6)	0.008 (1)	0
	$A_p \cos(\alpha_1)$	−0.0061 (6)	0.0052 (6)	−0.018 (1)	0
	$A_p \sin(\alpha_2)$	−0.0019 (7)	0.0040 (6)	−0.005 (1)	0
	$A_p \cos(\alpha_2)$	−0.0022 (7)	−0.0015 (6)	−0.005 (1)	0
	u_{11}, u_{22}, u_{33}	0.014 (2)	0.016 (2)	0.012 (1)	
	u_{12}, u_{13}, u_{23}	0.010 (1)	0.011 (1)	0.006 (1)	
O4	$\bar{p}$	0.2793 (4)	0.0542 (4)	0.5899 (8)	1
	$A_p \sin(\alpha_1)$	−0.0164 (6)	0.0403 (6)	−0.041 (1)	0
	$A_p \cos(\alpha_1)$	0.0423 (6)	0.0004 (6)	0.086 (1)	0
	$A_p \sin(\alpha_2)$	0.0071 (7)	−0.0024 (6)	0.017 (1)	0
	$A_p \cos(\alpha_2)$	−0.0025 (7)	0.0035 (6)	−0.009 (1)	0
	u_{11}, u_{22}, u_{33}	0.025 (2)	0.006 (1)	0.021 (2)	
	u_{12}, u_{13}, u_{23}	0.001 (1)	0.019 (2)	−0.002 (1)	
O5	$\bar{p}$	0.0533 (4)	0.7144 (4)	0.0418 (7)	1
	$A_p \sin(\alpha_1)$	0.0108 (6)	0.0538 (6)	0.024 (1)	0
	$A_p \cos(\alpha_1)$	−0.0093 (6)	−0.0070 (6)	−0.022 (1)	0
	$A_p \sin(\alpha_2)$	−0.0013 (7)	0.0076 (7)	−0.002 (1)	0
	$A_p \cos(\alpha_2)$	−0.0019 (7)	−0.0003 (7)	−0.004 (1)	0
	u_{11}, u_{22}, u_{33}	0.014 (2)	0.021 (2)	0.015 (1)	
	u_{12}, u_{13}, u_{23}	0.002 (1)	0.012 (1)	0.000 (1)	
Na1	$\bar{p}$	$\frac{1}{2}$	0	0	1
	$A_p \sin(\alpha_1)$	−0.0298 (6)	−0.0107 (6)	−0.084 (1)	0
	$A_p \cos(\alpha_1)$	0	0	0	0
	$A_p \sin(\alpha_2)$	0.0570 (6)	0.0444 (6)	0.145 (1)	0
	$A_p \cos(\alpha_2)$	0	0	0	0
	u_{11}, u_{22}, u_{33}	0.030 (2)	0.034 (2)	0.033 (2)	
	u_{12}, u_{13}, u_{23}	0.006 (1)	0.028 (2)	0.012 (1)	
Na2	$\bar{p}$	0	0.5100 (4)	$\frac{3}{4}$	1
	$A_p \sin(\alpha_1)$	0	0.0642 (5)	0	0
	$A_p \cos(\alpha_1)$	0.0046 (6)	0	0.003 (1)	0
	$A_p \sin(\alpha_2)$	0.0063 (6)	0	0.013 (1)	0
	$A_p \cos(\alpha_2)$	0	−0.0046 (6)	0	0
	u_{11}, u_{22}, u_{33}	0.026 (1)	0.018 (1)	0.022 (1)	
	u_{12}, u_{13}, u_{23}	0	0.020 (1)	0	
Na3	$\bar{p}$	0.2299 (3)	0.2207 (3)	0.1037 (7)	0.763 (7)
	$A_p \sin(\alpha_1)$	0.0055 (6)	0.0525 (5)	−0.011 (1)	0.373 (7)
	$A_p \cos(\alpha_1)$	0.0171 (4)	0.0035 (4)	0.0573 (8)	−0.093 (7)
	$A_p \sin(\alpha_2)$	−0.0065 (4)	0.0035 (4)	−0.0203 (8)	0.046 (8)
	$A_p \cos(\alpha_2)$	0	0	0	0.257 (7)
	u_{11}, u_{22}, u_{33}	0.014 (1)	0.013 (1)	0.021 (1)	
	u_{12}, u_{13}, u_{23}	0.0015 (8)	0.013 (1)	−0.0003 (9)	
Na4	$\bar{p}$	0	0.0194 (6)	$\frac{3}{4}$	0.386 (8)
	$A_p \sin(\alpha_1)$	0	0	0	−0.55 (1)
	$A_p \cos(\alpha_1)$	−0.035 (1)	0	−0.083 (2)	0
	$A_p \sin(\alpha_2)$	0	0	0	0
	$A_p \cos(\alpha_2)$	0	0	0	−0.17 (1)
	u_{11}, u_{22}, u_{33}	0.018 (3)	0.010 (2)	0.020 (3)	
	u_{12}, u_{13}, u_{23}	0	0.015 (3)	0	

correlations between some parameters and the degeneration of some thermal ellipsoids during the refinement in the noncentrosymmetric model, pointed towards a preference for the centrosymmetric model. It is more convenient to pass over to a non-standard, strongly oblique-angled basic monoclinic cell with the parameters $\mathbf{a}' = \mathbf{a}_M - \mathbf{c}_M$, $\mathbf{b}' = \mathbf{b}_M$, $\mathbf{c}' = \mathbf{c}_M$, $\beta' = 144.45°$. The modulation vector $\mathbf{q} = 0.2\mathbf{c}'^*$ now has only one component and the calculations can be essentially reduced. The structure was refined in the new cell, but the ultimate coordinates were recalculated on a standard basis. The results of the refinement of the structural parameters of NTP are listed in Table 2.

Discussion

The monoclinic modification of $NaTiP_2O_9$ is based on $\{Ti_2[PO_4]_4O_2\}_\infty$ complex studies, such as the high-temperature orthorhombic phases we studied at 573, 663 and 743 K (Maximov, Klokova, Verin & Timofeeva, 1990; Bolotina, Maximov, Tamazyan & Klokova, 1993; Klokova, Maximov & Tamazyan, 1993). Each infinite complex is built up of chains of Ti and P tetrahedra. The chains run through the crystal parallel to the c axis. The connection of such chains into one three-dimensional framework is achieved by polyhedra of Na_1 and Na_2 cations (Fig. 3). The sites of these Na atoms are completely occupied in all the phases we studied at 573, 663 and 723 K. Other Na atom sites, in our case the Na3 and Na4 sites, are located in rather spacious channels of the crystal structure. The corresponding sites in the high-temperature superionic phases of $Na_4TiP_2O_9$ are occupied statistically by Na atoms which play an active part in ionic transport. The Na3 and Na4 atom sites in the monoclinic phase were also considered to be statistically occupied, with the occupation modulation.

A detailed analysis of the modulation parameters (Table 2) shows that the atomic shifts are significant for all the atoms of the structure. For most atoms the main shifts are oriented along the [010] direction. For O4 and O5, which form the periphery of the radicals $\{Ti_2[PO_4]_4O_2\}_\infty$ (empty tops of the P tetrahedra), as for all Na atoms, the amplitudes of the atomic shifts are also significant in other directions. Also notable are the large amplitudes of the occupancy modulations of the Na3 and Na4 sites, *i.e.* atoms located in conductivity channels. The supercell consists of 5 × 5 subcells, but there are only five different types of subcells. Their arrangement in the supercell is presented in Fig. 4. Figs. 5(*a–e*) show the location of the Na and O atoms in one of the largest voids of the $Na_4TiP_2O_9$ structure for the various types of subcells. These voids form the main conductivity channels in the [001] direction (in Fig. 3 these voids are shown by point shading). Fig. 5 provides three digits in atomic labelling: the first digit is the atomic number according to Table 2, the second is the number of the subcell in the **c** direction and the third corresponds to the number of the subcell in the **a** direction. For example, the label Na411 in Fig. 5(*a*) indicates the Na4 atom in the subcell which lies in the upper left corner of the supercell shown in Fig. 4, *i.e.* in the subcell of type 1. The Na314 atom in the same picture is connected to the 'true' Na314 atom by a symmetry transformation. The Na4···O and Na4···Na3 interatomic distances and their correlation with occupancy modulations of Na atom sites are presented in Table 3. Inside the conductivity channels there are Na4 atoms with the mean occupancy coefficient $q_{Na4} = 0.39$. Na3 atoms, which are located in the voids surrounding the main conductiv-

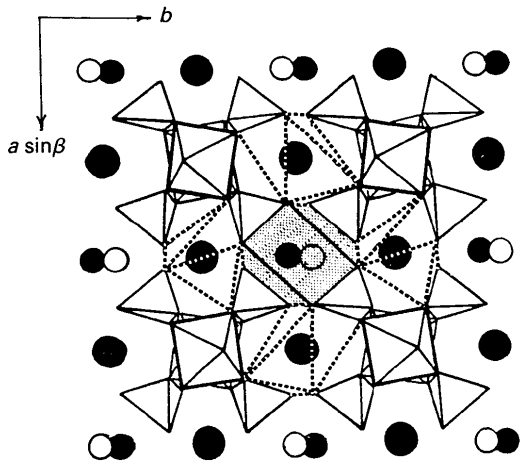

Fig. 3. Crystal structure of the monoclinic modification of $Na_4TiP_2O_9$. The empty octahedra represent TiO_6 octahedra, whilst the empty tetrahedra represent the PO_4 tetrahedra. These two form infinite chains in the [001] direction of the composition $\{Ti_2[PO_4]_4O_2\}_\infty$. The octahedra with broken lines are populated by Na1 and Na2 atoms; Na atoms are given by large solid circles. The shaded distorted orthorhombic prisms represent the conductivity channels occupied by Na4, given by small solid and open circles; Na3 atoms are not indicated.

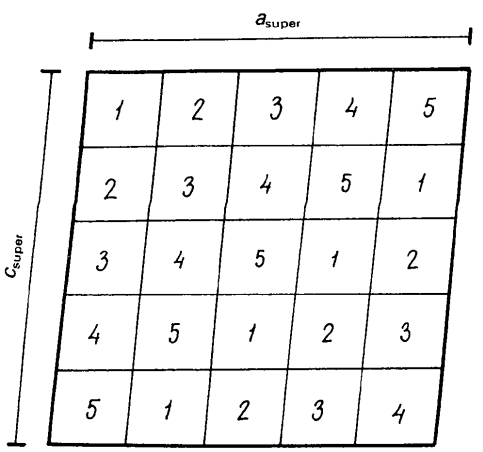

Fig. 4. Arrangement of the various types of subcell in a superstructural cell, $5a \times b \times 5c$, of $Na_4TiP_2O_9$.

Table 3. *Interatomic distances in* Na4 *polyhedra and* Na3—Na4 *distances* (Å)

Site occupancy coefficients for Na atoms are shown in square brackets.

Na411 [0.88]	O414	2.30 (3)	Na421 [0.88]	O455	2.30 (3)
	O515	2.33 (4)		O524	2.33 (4)
	O415	2.39 (3)		O424	2.39 (3)
	O514	2.50 (4)		O555	2.50 (4)
	O411	3.01 (4)		O452	3.01 (4)
	O512	3.16 (4)		O553	3.16 (4)
	O412	3.23 (3)		O421	3.23 (3)
	O513	3.25 (3)		O522	3.25 (3)
Na411 [0.88]	Na312 [0.12]	2.57 (3)	Na421 [0.88]	Na353 [0.12]	2.57 (3)
	Na313 [0.81]	3.24 (3)		Na322 [0.81]	3.24 (3)
	Na315 [1.0]	3.44 (4)		Na324 [1.0]	3.44 (4)
	Na314 [0.95]	3.47 (3)		Na355 [0.95]	3.47 (3)
Na431 [0.08]	O534	2.55 (3)	Na441 [0.00]	O533	2.79 (3)
	O445	2.59 (4)		O542	2.79 (3)
	O543	2.85 (4)		O444	2.86 (3)
	O434	2.94 (4)		O435	2.86 (3)
	O532	2.94 (4)		O544	2.94 (4)
	O545	3.01 (3)		O535	2.94 (4)
	O442	3.04 (4)		O432	3.09 (4)
	O431	3.32 (3)		O441	3.09 (4)
Na431 [0.08]	Na343 [0.90]	2.27 (3)	Na441 [0.00]	Na335 [0.12]	2.85 (3)
	Na345 [0.81]	3.03 (4)		Na344 [0.12]	2.85 (3)
	Na334 [0.90]	3.13 (4)		Na342 [1.0]	2.89 (4)
	Na332 [1.0]	3.33 (3)		Na333 [1.0]	2.89 (4)
Na451 [0.08]	O525	2.55 (3)			
	O454	2.59 (4)			
	O552	2.85 (4)			
	O425	2.94 (4)			
	O523	2.94 (4)			
	O554	3.01 (3)			
	O451	3.04 (4)			
	O422	3.32 (3)			
Na451 [0.08]	Na352 [0.90]	2.27 (3)			
	Na354 [0.81]	3.03 (4)			
	Na325 [0.90]	3.13 (4)			
	Na323 [1.0]	3.33 (3)			

ity channels, have a mean occupancy coefficient $q_{Na3} = 0.76$.

It is evident from Fig. 5 and Table 3 that in each type of subcell, the geometric configurations of the voids which form the conductivity channels differ slightly from each other. Besides the geometric configurations of the voids, the occupancy coefficients of the corresponding Na atom sites both inside the channels and the surrounding voids also change. From Table 3 we can derive that in the monoclinic modification, almost fully occupied Na atom sites exist among those which are statistically populated in the high-temperature superionic state. This is most evident for Na4 atoms. In three out of five subcells, the occupancy for Na4 atoms is close to 0; in the other two cells it is close to unity. In Fig. 5 the solid circles indicate almost fully occupied Na sites, the open circles indicate almost empty Na sites. It should be noted that at $q_{Na4} = 0.88$ (two subcells out of five), there are only four oxygen atoms in the closest oxygen coordination of the Na4 atom, Na4—O distances being 2.30 (3)–2.50 (3) Å. In this case of a clearly manifested tetrahedral coordination of Na atoms, the dimensions of the conductivity windows are strongly reduced, which results in congestion of the main conductivity channels in the monoclinic structure of $Na_4TiP_2O_9$ crystals. We tested the structure model, in which the Na3 and Na4 sites are either vacant or fully occupied. To describe modulations of these site occupancies during the refinement of the structure, we used step modulation functions, taking values of occupation of either 0 or 1. In this case, Na3 atoms occupy four out of five subcells, while Na4 atoms occupy two out of five. The R factors of the refinement of such a model are only slightly larger than in the two-harmonic model (therefore, for second-order satellites $R_2 \sim 13\%$) and, in our opinion, this model is quite acceptable for the description of the structure.

We are most thankful to Dr R. Tamazyan for valuable discussions at all stages during this research and to Dr R. Neder for discussion of the results and helping in the translation of the manuscript.

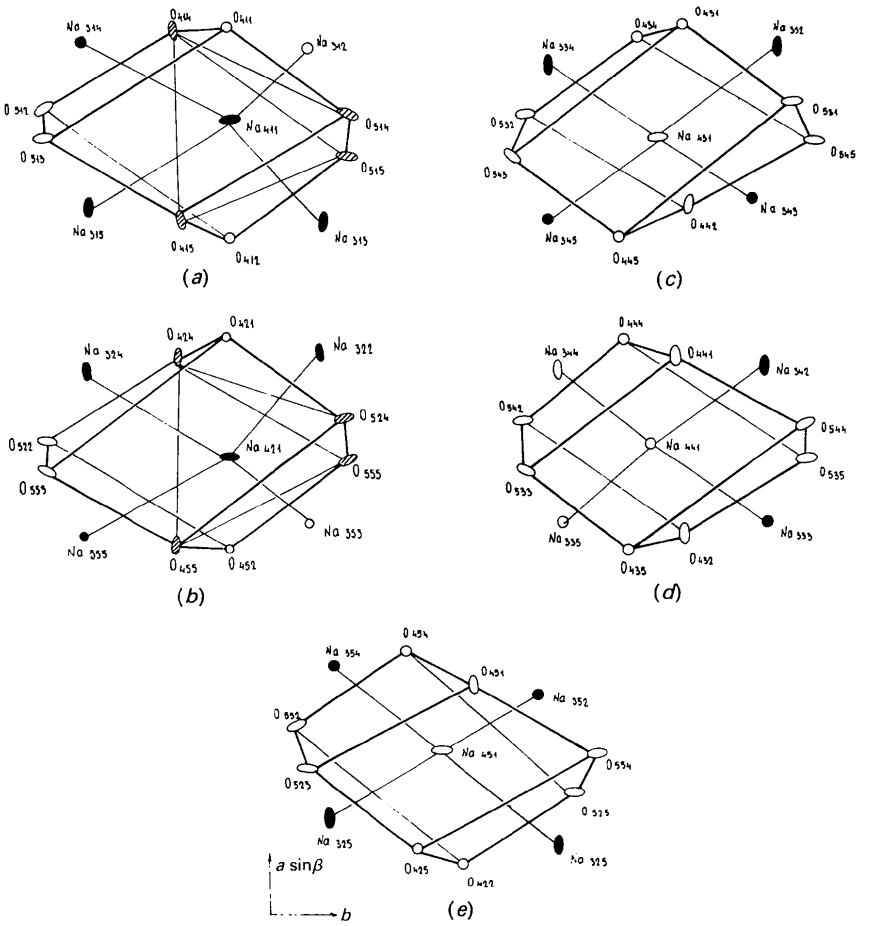

Fig. 5. Atomic arrangement of the large voids which form the conductivity channels in the [001] direction, the arrangement of Na atoms inside these voids (Na4) and the surrounding of these voids (Na3) for the various type of the subcells: (*a*) 1st type subcell; (*b*) 2nd type subcell: (*c*) 3rd type subcell; (*d*) 4th type subcell; (*e*) 5th type subcell.

This work has been financially supported by the Alexander von Humboldt Foundation and by the Russian Fundamental Investigations Foundation, Grant No. 93-02-2002.

References

BOLOTINA, N. B., MAXIMOV, B. A., TAMAZYAN, R. A. & KLOKOVA, N. E. (1993). *Kristallographiya*, **38**(4), 51–55.
FRIEDEL, G. (1964). *Lecons de Cristallographie* (1926). Reprinted. Paris: A. Blanchard.
IVANOV-SHITS, A. K. & SIGARYOV, S. E. (1990). *Solid State Ionics*, **40/41**, 76–78.
KLOKOVA, N. E., MAXIMOV, B. A. & TAMAZYAN, R. A. (1993). *Kristallographiya*, **38**(4), 56–60.
MATSAJUKI, F., KATSU, O. & SIMMI, A. (1983). Japanese Patent COIB 25/45, HOIB 1/06 N. 56-109064. Published 28 January.
MAXIMOV, B., BOLOTINA, N. & SCHULZ, H. (1994). *Z. Kristallogr.* Submitted.
MAXIMOV, B., KLOKOVA, N. E., VERIN, I. A. & TIMOFEEVA, V. A. (1990). *Kristallographiya*, **35**(4), 847–851.
PETŘIČEK, V. (1993). *JANA92 User's Guide*. Prague: Academy of Sciences of the Czech Republic.
PETŘIČEK, V. & COPPENS, P. (1988). *Acta Cryst.* A**44**, 1051–1055.
PETŘIČEK, V., COPPENS, P. & BECKER, P. (1985). *Acta Cryst.* A**41**, 478–483.
WOLFF, P. M. DE (1974). *Acta Cryst.* A**30**, 777–785.
WOLFF, P. M. DE, JANSSEN, T. & JANNER, A. (1981). *Acta Cryst.* A**37**, 625–636.
YAMAMOTO, A. (1982). *Acta Cryst.* A**38**, 87–92.

Acta Cryst. (1994). B**50**, 268–279

Structural, Vibrational and Electronic Properties of a Crystalline Hydrate from *ab initio* Periodic Hartree–Fock Calculations

BY LARS OJAMÄE AND KERSTI HERMANSSON

Institute of Chemistry, Uppsala University, Box 531, *S*-751 21 *Uppsala, Sweden*

AND CESARE PISANI, MAURO CAUSÀ AND CARLA ROETTI

Department of Inorganic, Physical and Materials Chemistry, University of Torino, via Giuria 5, *I*-10125 *Torino, Italy*

(*Received* 6 *February* 1993; *accepted* 27 *September* 1993)

Abstract

The hydrate crystal lithium hydroxide monohydrate $LiOH.H_2O$ has been studied by *ab initio* periodic Hartree–Fock calculations. The influence of the crystalline environment on the local molecular properties (molecular geometry, atomic charges, electron density, molecular vibrations and deuterium quadrupole coupling constants) of the water molecule, the lithium and hydroxide ions has been calculated. A number of crystalline bulk properties are also presented; optimized crystalline structure, lattice energy and electronic band structure. The optimized cell parameters from calculations with a large basis set of triple-zeta quality differ by only 1–3% from the experimental neutron-determined cell, whereas the STO-3g basis set performs poorly (differences of 5–10%). With the triple-zeta basis also the atomic positions and intermolecular distances agree very well with the experiment. The lattice energy differs by ~8% from the experimental value, and by at most 3% when a density-functional electron correlation correction is applied. Large electron-density rearrangements occur in the water molecule and in the hydrogen bond and are in qualitative and quantitative agreement with experimental X-ray diffraction results. The quadrupole-coupling constants of the water and hydroxide deuterium atoms are found to be very sensitive to the O—H bond length and are in good agreement with experimental values when the calculation is based on the experimental structure. The anharmonic O—H stretching vibrations in the crystal are presented and found to be very close to results from calculations on molecular clusters. The electronic band and density-of-states spectra are discussed. Model calculations on a hydrogen fluoride chain were used to rationalize the results.

Introduction

The water molecule and its unique binding properties are of interest to both experimentalists and theoreticians. Crystalline hydrates have consequently been extensively characterized experimentally. The effect of the crystalline environment on the structure, vibrations, electron density, quadrupolar coupling constants *etc.* of the water molecule have been investigated in many hundreds of diffraction and spectroscopic studies (*e.g.* Falk & Knop, 1973;

©1994 International Union of Crystallography
Printed in Great Britain – all rights reserved